

## Efficient CO<sub>2</sub> Electroreduction to N-propanol on Matching Cobalt Phthalocyanine/Copper Tandem Catalyst

Chunjun Chen,<sup>a, b\*</sup> Min Wang,<sup>a, b</sup> Yichi Zhang,<sup>a, b</sup> Xue Yang,<sup>c</sup> Kang Zou,<sup>c\*</sup> Wei Lin,<sup>c\*</sup> Mingyuan He,<sup>a, b</sup> Haihong Wu,<sup>a, b</sup> and Buxing Han<sup>a, b, d \*</sup>

a. Shanghai Key Laboratory of Green Chemistry and Chemical Processes, State Key Laboratory of Petroleum Molecular & Process Engineering, School of Chemistry and Molecular Engineering, East China Normal University, Shanghai, 200062, China.

b. Institute of Eco-Chongming, Chongming District, Shanghai, 202162, China.

c. State Key Laboratory of Petroleum Molecular and Process engineering, SKLPMPE, Sinopec research institute of petroleum processing Co., LTD., Beijing 100083, China.

d. Beijing National Laboratory for Molecular Sciences, CAS Key Laboratory of Colloid and Interface and Thermodynamics, CAS Research/Education Center for Excellence in Molecular Sciences, Center for Carbon Neutral Chemistry, Institute of Chemistry, Chinese Academy of Sciences, Zhongguancun North First Street 2, Beijing, 100190, P. R. China.

## Experimental Section

**Materials:** Tetrahydrofuran (A. R. grade), dichloromethane (A. R. grade), Acetonitrile (A. R. grade), and Ni foam were obtained from Sinopharm Chem. Reagent Co. Ltd. Cobalt Phthalocyanine (99%), KOH (85%), Triethylamine (99.7%), Sodium 2, 2-dimethyl-2-silapentane-5-sulfonate (DSS, 99%), and Phenol were purchased from Alfa Aesar China Co., Ltd. D<sub>2</sub>O (99.8% D) was obtained from Innochem Co., Ltd. N<sub>2</sub> (99.999%) and CO<sub>2</sub> (99.999%) were provided by Beijing Analytical Instrument Company. Deionized water was used in the experiments.

**Synthetic procedures for CoPc electrode:** Firstly, the CoPc (0.25mg) was dissolved in the DCM (1mL) under ultrasonic. Then 3 mg of active carbon and 40  $\mu$ L of Nafion ionomer solution (5 wt% in H<sub>2</sub>O) were added into the above solution and sonicated for 30 min. Then, the obtained slurry (0.2 mL) was slowly drop cast onto a porous hydrophobic carbon paper at 80 °C. The CoPc load on the carbon paper is approximately 0.05mg/cm<sup>2</sup>.

**Synthetic procedures for CoPc-THF electrode:** The Synthetic procedure for CoPc-THF electrode was similar with that of CoPc electrode except that the DCM was replaced by the mixed solvent. For the CoPc-THF, the mixed solvent was composed of DCM and THF, the volume ratio of DCM and THF was 9:1. Firstly, the CoPc (0.25mg) was dissolved in the mixed solvent of DCM and THF (1 mL, 9:1). Then, the mixture was ultrasonically treated for 1 h under 25°C. Then 3 mg of active carbon and 40  $\mu$ L of Nafion ionomer solution (5 wt% in H<sub>2</sub>O) were added into the above solution and sonicated for 30 min. Then, the obtained slurry (0.2 mL) was slowly drop cast onto a porous hydrophobic carbon paper at 80 °C. The CoPc-THF load on the carbon paper is approximately 0.05 mg/cm<sup>2</sup>.

**Synthetic procedures for CuO:** CuO was fabricated through the annealing of Cu(OH)<sub>2</sub> nanorods under N<sub>2</sub> atmosphere. Firstly, the Cu(OH)<sub>2</sub> were prepared by a reported method.<sup>[S1]</sup> Typically, 1 g of Cu(NO<sub>3</sub>)<sub>2</sub> was dissolved in 100 mL distilled water. Then, 30 mL NH<sub>3</sub>·H<sub>2</sub>O (0.15 M) solution was added to the Cu(NO<sub>3</sub>)<sub>2</sub> solution under stirring at room temperature. A blue precipitate of Cu(OH)<sub>2</sub> was produced when 10 mL of NaOH (1 M) solution was dropwise added ( $\approx 2$  mL min<sup>-1</sup>) to the above solution to adjust the pH value to 9-10. After 30 min, the blue Cu(OH)<sub>2</sub> precipitate was centrifuged and washed several times with H<sub>2</sub>O to obtain a solid product, which was dried by freeze-drying for 24 h. Secondly, the CuO was prepared by annealing the Cu(OH)<sub>2</sub> in the N<sub>2</sub> atmosphere at 300 °C for 2 h with a heating rate of 20 °C min<sup>-1</sup>.

**Synthetic procedures for CuO, CoPc/CuO and CoPc-THF/CuO electrode:** For the CuO electrode, a catalyst slurry that contained 5 mg of CuO, 1 mL of methanol and 20  $\mu$ L of Nafion ionomer solution (5 wt% in H<sub>2</sub>O) was first mixed and sonicated for 30 min. Then, the catalyst slurry (0.2 mL) was slowly drop cast onto a PTFE membrane (Fuel Cell Store) under vacuum. The CuO electrode was obtained. For the CoPc/CuO, 1 mL of CuO catalysts slurry and 0.2 mL of CoPc catalysts slurry was mixed and sonicated for 30 min. Then, the mixed catalyst slurry (0.2 mL)

was slowly drop cast onto a PTFE membrane under vacuum. The CoPc/CuO electrode was obtained. For the CoPc-THF/CuO, 1 ml of CuO catalysts slurry and 0.2 mL of CoPc-THF catalysts slurry was mixed and sonicated for 30 min. Then, the mixed catalyst slurry (0.2 mL) was slowly drop cast onto a PTFE membrane under vacuum. The CoPc-THF/CuO electrode was obtained.

**Synthetic procedures for OD-CuO, CoPc/OD-Cu and CoPc-THF/OD-Cu electrode:** The OD-CuO, CoPc/OD-Cu and CoPc-THF/OD-Cu were obtained by electroreduction of CuO, CoPc/CuO and CoPc-THF/CuO at a constant voltage of -1 V vs. RHE for 10 min.

**Characterization.** The SEM characterization was carried out using a HITACHI S-4800. X-ray photoelectron spectroscopy (XPS) study was performed on the Thermo Scientific ESCALab 250Xi using a 200W Al-K $\alpha$  radiation. In the analysis chamber, the base pressure was about  $3 \times 10^{-10}$  mbar. Typically, the hydrocarbon C1s line at 284.8 eV from adventitious carbon was used for energy referencing. The X-ray adsorption spectroscopy (XAS) measurements were performed at the 1W1B beamline at Beijing Synchrotron Radiation Facility (BSRF). The ultraviolet–visible (UV-Vis) absorption spectrum was measured using a Lambda 1050.

**XAFS measurements.** The X-ray absorption fine structure spectra data (Co K-edge) were collected at 1W1B station in Beijing Synchrotron Radiation Facility (BSRF, operated at 2.5 GeV with a maximum current of 250 mA). The data were collected in fluorescence excitation mode using a Lytle detector.

The acquired EXAFS data were processed according to the standard procedures using the Athena and Artemis implemented in the IFEFFIT software packages. The fitting detail is described below:

The acquired EXAFS data were processed according to the standard procedures using the ATHENA module implemented in the IFEFFIT software packages. The EXAFS spectra were obtained by subtracting the post-edge background from the overall absorption and then normalizing with respect to the edge-jump step. Subsequently, the  $\chi(k)$  data were Fourier transformed to real (R) space using a hanning windows ( $dk=1.0 \text{ \AA}^{-1}$ ) to separate the EXAFS contributions from different coordination shells. To obtain the quantitative structural parameters around central atoms, least-squares curve parameter fitting was performed using the ARTEMIS module of IFEFFIT software packages.

The following EXAFS equation was used:

$$\chi(k) = \sum_j \frac{N_j S_o^2 F_j(k)}{k R_j^2} \exp[-2k^2 \sigma_j^2] \exp\left[\frac{-2R_j}{\lambda(k)}\right] \sin[2k R_j + \phi_j(k)]$$

$S_0^2$  is the amplitude reduction factor,  $F_j(k)$  is the effective curved-wave backscattering amplitude,  $N_j$  is the number of neighbors in the  $j^{th}$  atomic shell,  $R_j$  is the distance between the X-ray absorbing central atom and the atoms in the  $j^{th}$  atomic shell (backscatterer),  $\lambda$  is the mean free path in Å,  $\phi_j(k)$  is the phase shift (including the phase shift for each shell and the total central atom phase shift),  $\sigma_j$  is the Debye-Waller parameter of the  $j^{th}$  atomic shell (variation of distances around the average  $R_j$ ). The functions  $F_j(k)$ ,  $\lambda$  and  $\phi_j(k)$  were calculated with the ab initio code FEFF8.2. The obtained  $S_0^2$  was fixed in the subsequent fitting. The coordination number N, interatomic distance (R), Debye-Waller factor  $\sigma^2$ , and the edge-energy shift  $\Delta E_0$  were allowed to run freely.

**Electrochemical study.** Electrochemical studies were conducted in an electrochemical flow cell which including a gas chamber, a cathodic chamber, and an anodic chamber, as reported in our previous work.<sup>[S2]</sup> The dimension of the gas chamber, cathodic chamber, and anodic chamber were the same, which was  $1.5 \times 0.7 \times 1$  cm. The distance between electrode and membrane was 1 cm and the electrode area was 1.05 cm<sup>2</sup>. The silicone gaskets (1mm) were placed between each component for sealing and the device was tightened using four bolts. An anion exchange membrane (FumasepFAA-3-PK-130) was used to separate the anodic and cathodic chambers, the Ni foam were used as the counter electrodes, respectively. The electrolysis was conducted using a CHI 660e electrochemical workstation equipped with a high current amplifier CHI 680c. Saturated Ag/AgCl was used as the reference and it was calibrated with respect to RHE:  $E \text{ (versus RHE)} = E \text{ (versus Ag/AgCl)} + 0.197 \text{ V} + 0.0591 \text{ V/pH} \times \text{pH}$ . For performance studies, 1 M KOH was used as the electrolyte, and it was circulated through the cathodic and anodic chambers using peristaltic pumps at a rate of 20 mL min<sup>-1</sup>. The flow rate of CO<sub>2</sub> gas through the gas chamber was controlled to be 20 sccm using a digital gas flow controller. The IR compensation was used for potential correction in electrochemical testing.

**Product analysis.** The gaseous product of electrochemical experiments was collected using a gas bag and analyzed by gas chromatography (GC, HP 4890D), which was equipped with TCD detectors using argon as the carrier gas. The liquid product was analyzed by <sup>1</sup>H NMR (Bruker Avance III 400 HD spectrometer) in deuterioxide.

### **Calculations of Faradaic efficiencies of gaseous and liquid products.**

#### **liquid products:**

After electrolysis, a certain amount of internal standard solution was added to the electrolyte as the internal standard. Because the concentration of internal standard was known, the moles of liquid products can be calculated from integral areas and calibration curves. To accurately integrate the products in NMR analysis, two standards located in different regions were used in NMR analysis. The sodium 2, 2-dimethyl-2-silapentane-5-sulfonate (DSS) was the reference for n-propanol, ethanol and acetic acid, and the phenol was the reference for formate. 400 µL catholyte

after the reaction was mixed with 100  $\mu$ L 6 mM DSS solution, 100  $\mu$ L 200 mM phenol and 200  $\mu$ L D<sub>2</sub>O, and then analyzed by <sup>1</sup>H NMR (Bruker Avance III 400 HD spectrometer).

The Faradaic efficiency(FE) of liquid product is:

$$FE = \frac{n(\text{moles of product})}{Q / NF} \times 100\%$$

(Q: charge (C); F: Faradaic constant (96485 C/mol); N: the number of electrons required to generate the product; n: the moles of product)

For the HCOOH, CH<sub>3</sub>COOH, CH<sub>3</sub>CH<sub>2</sub>OH and n-C<sub>3</sub>H<sub>7</sub>OH, the N are 2, 8, 12 and 18 respectively.

### **Gaseous products:**

The gas products were collected by using the gas bag. A 5-minute electrolysis was conducted to gain the steady state before the collection of the gas products, and the collection time was 10 min. .

The Faradaic efficiency(FE) of gaseous product is:

$$FE = \frac{n(\text{moles of product})}{Q / NF} \times 100\%$$

(Q: charge (C); F: Faradaic constant (96485 C/mol); N: the number of electrons required to generate the product; n: the moles of products)

For the H<sub>2</sub>, CO and CH<sub>4</sub>, the N are 2, 2 and 8 respectively.

From the GC peak areas and calibration curves, we could obtain the V % of gaseous products. The flow rate of the gas outlet (v) can be measured, then the moles of gaseous products could be calculated:

### **Computational Method**

All DFT calculations were performed using Vienna Ab initio Simulation Package (VASP).<sup>[S3]</sup> The projector augmented wave (PAW) pseudopotential<sup>[S4]</sup> with the PBE generalized gradient approximation (GGA) exchange correlation function<sup>[S5]</sup> was utilized in the computations. The cutoff energy of the plane waves basis set was 500 eV and a Monkhorst-Pack mesh of 2×2×1 was used in K-sampling in the adsorption energy calculation. All atoms were fully relaxed with the energy convergence tolerance of 10<sup>-5</sup> eV per atom, and the final force on each atom was < 0.05 eV Å<sup>-1</sup>.

All periodic slabs have a vacuum layer of at least 15 Å. The bottom layer of atoms was fixed at their optimized bulk-truncated positions during geometry optimization, and the rest of atoms could relax.

We used standard CoPc molecules as the initial DFT calculation model, and to ensure that the molecules are not affected by periodic unit cells, a minimum of 8 Å vacuum layer is guaranteed. Meanwhile, THF is modified at the

bottom-site of Co, and reactive species are considered to adsorb at the top-site of Co.

The adsorption energy of reaction intermediates, can be computed using the following Equation (1):

$$\Delta E = E_{\text{ads}} - E^* \quad (1)$$

$$\Delta G = \Delta E + \Delta E_{\text{ZPE}} - T\Delta S \quad (2)$$

Where  $\Delta E_{\text{ZPE}}$  is the zero-point energy change,  $\Delta S$  is the entropy change. In this work, the values of  $\Delta E_{\text{ZPE}}$  and  $\Delta S$  were obtained by vibration frequency calculation.

The  $\Delta G$  at different voltages can be obtained based on the  $\Delta G$  at 0V. The calculation of  $\Delta G$  at different voltages follows this formula:  $\Delta G = \Delta G(0V) + N(\text{transfer electron number}) * \text{bias voltages}$ .

## Supplementary Figures

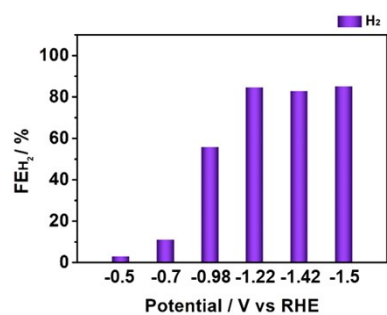


**Figure S1.** The FE of H<sub>2</sub> over CoPc at different potentials.

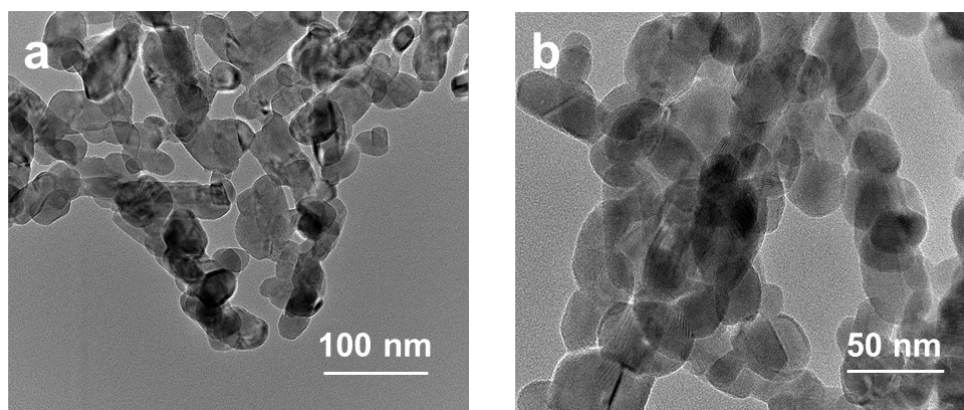


**Figure S2.** (a, b) The TEM images of CuO.



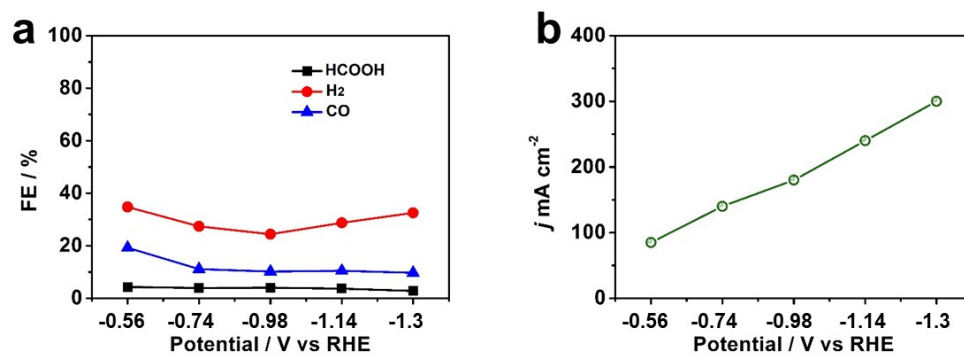


**Figure S3.** (a) The FE of C1 products at different potentials over OD-Cu during CO<sub>2</sub>RR. (b) The current density at different potentials over OD-Cu during CO<sub>2</sub>RR.

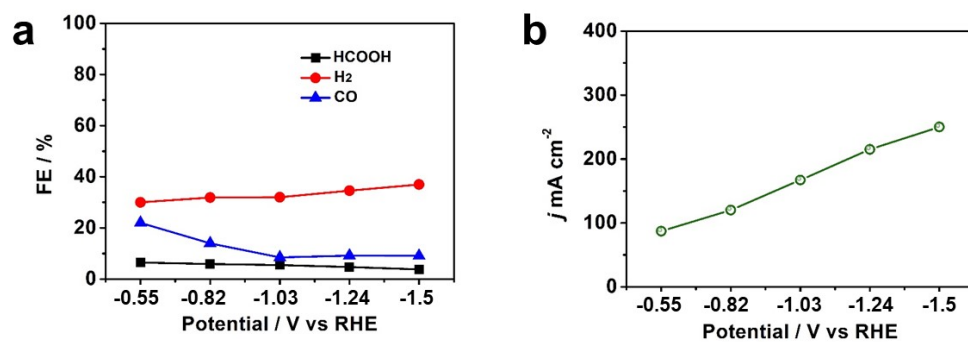


**Figure S4.** (a) The FE of C1 products at different potentials over CoPc/OD-Cu during CO<sub>2</sub>RR. (b) The current density at different potentials over CoPc/OD-Cu during CO<sub>2</sub>RR.

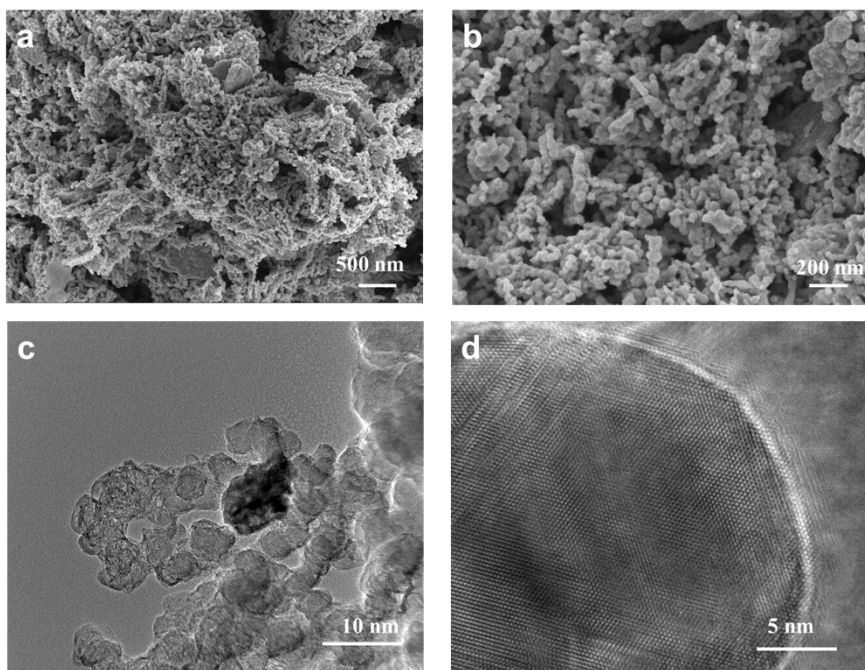


**Figure S5.** (a, b) The SEM images of CoPc-THF/OD-Cu. (c, d) The TEM images of CoPc-THF/OD-Cu.

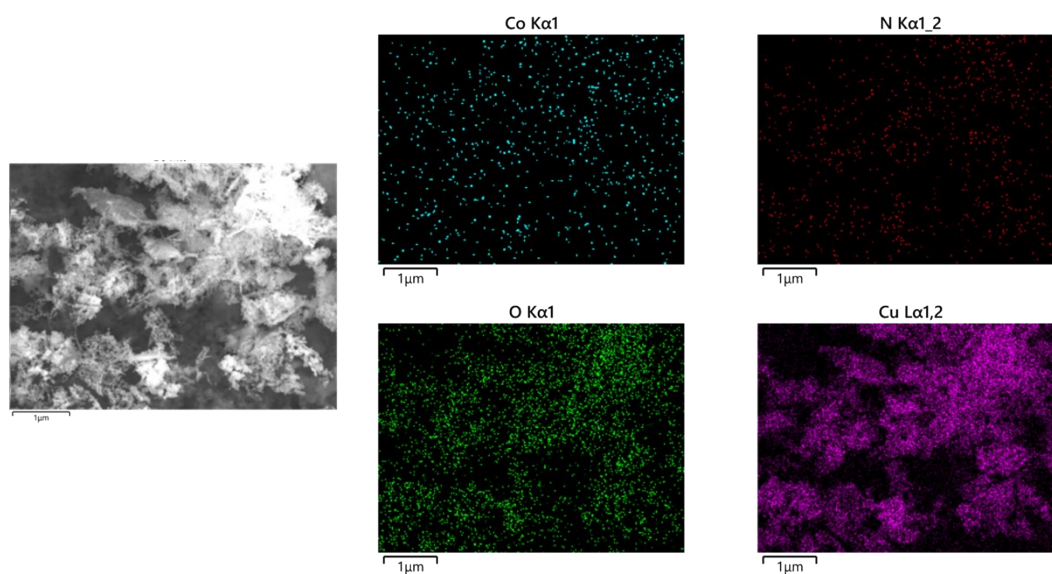


**Figure S6.** The energy dispersive X-ray spectroscopy CoPc-THF/OD-Cu.

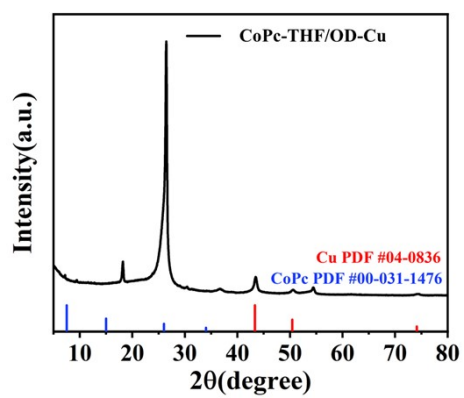


**Figure S7.** The XRD pattern of CoPc-THF/OD-Cu.

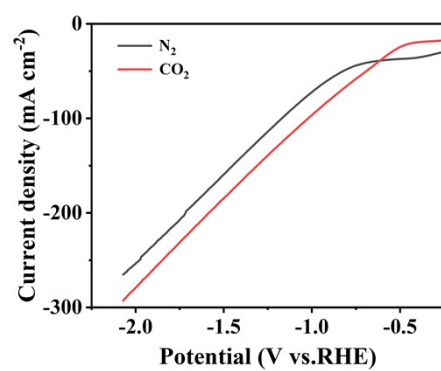


**Figure S8.** The LSV curves over CoPc-THF/OD-Cu under CO<sub>2</sub> and N<sub>2</sub> atmosphere.

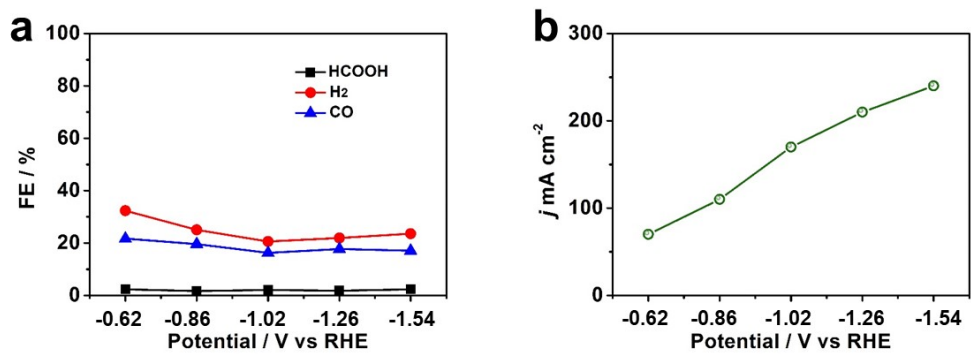


**Figure S9.** (a) The FE of C1 products at different potentials over CoPc-THF/OD-Cu during CO<sub>2</sub>RR. (b) The current density at different potentials over CoPc-THF/OD-Cu during CO<sub>2</sub>RR.

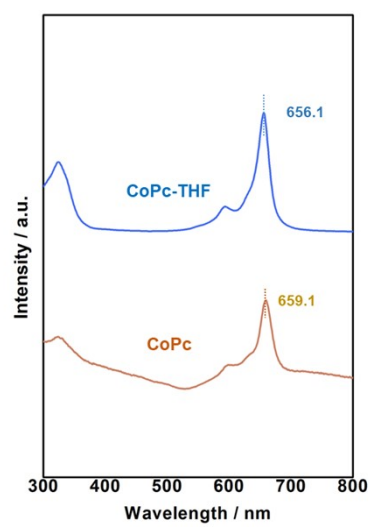


**Figure S10.** The ultraviolet–visible (UV-Vis) absorption spectrum of CoPc and CoPc-THF solution.



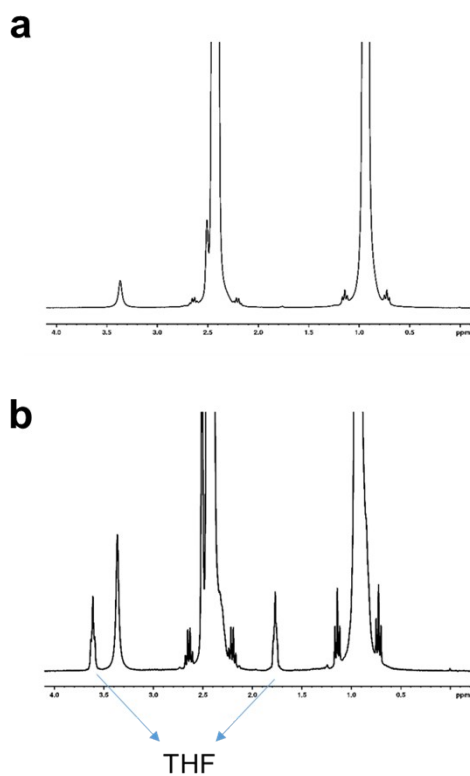


**Figure S11.** (a) <sup>1</sup>H NMR spectra of the triethylamine. (b) <sup>1</sup>H NMR spectra of the extract liquor from the CoPc-THF.

To verify the THF coordination with CoPc during CO<sub>2</sub>RR, after a 30 min electrolysis, the CoPc molecules on the cathode electrode were dissolved by dimethylsulfoxide (DMSO) and then subjected to spectroscopic characterization. To replace the THF that coordinated with CoPc, triethylamine was added to the DMSO solution, because the triethylamine exhibits stronger coordination with CoPc.

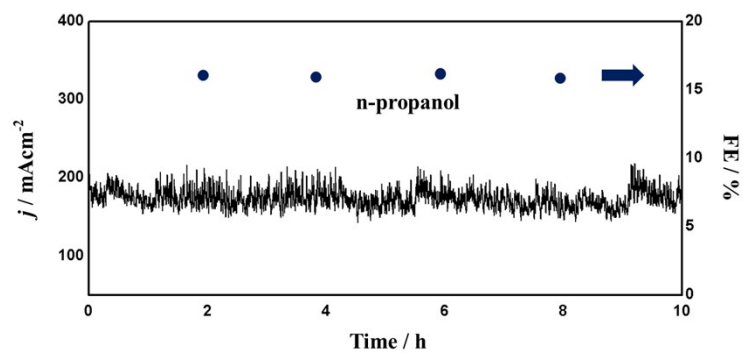


**Figure S12.** The current density and FE of n-propanol on CoPc-THF/OD-Cu at -1 V vs. RHE with 10-hour potentiostatic electrolysis tests.

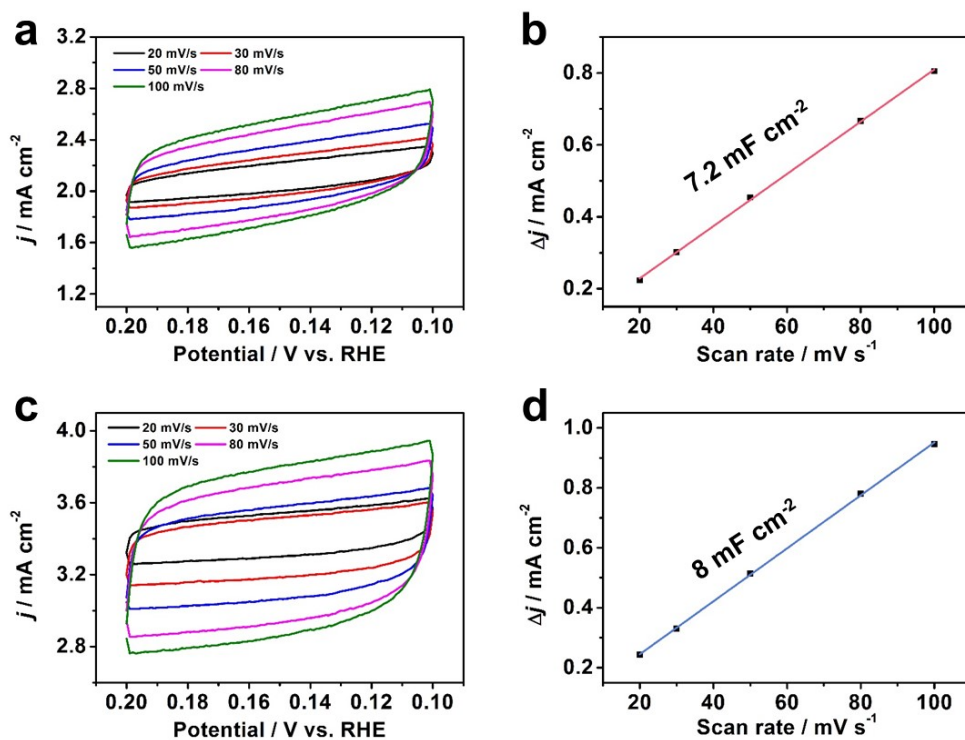


**Figure S13.** (a) The cyclic voltammetry at different scan rates over CoPc. (b) The charging current density differences plotted against the scan rates over CoPc. (c) The cyclic voltammetry at different scan rates over CoPc-THF. (d) The charging current density differences plotted against the scan rates over CoPc-THF.

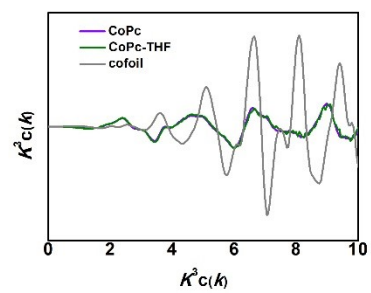


**Figure S14.** Co K-edge extended XAFS oscillation function  $k^3w(k)$  for different catalysts.

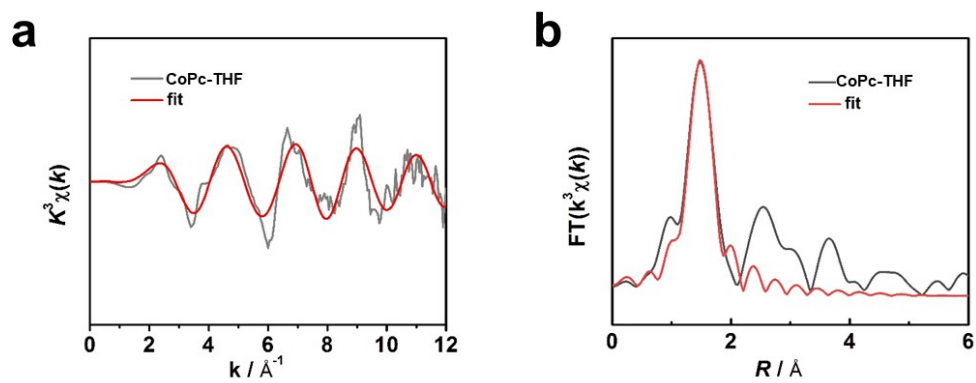


**Figure S15.** The EXAFS data fitting results of CoPc-THF.

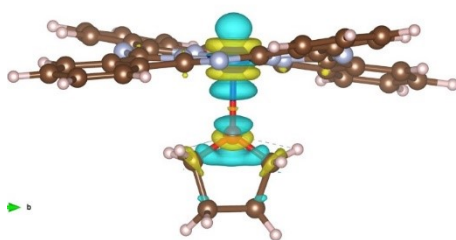


**Figure S16.** The charge density differences of the CoPc/THF. (Yellow represents electron accumulation and blue represents electron depletion).

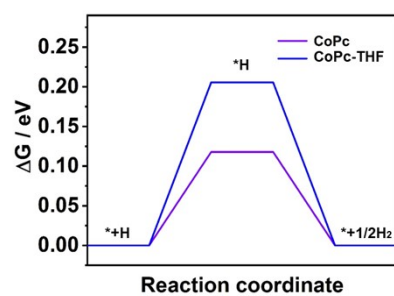


**Figure S17.** Reaction Gibbs free energy diagrams for HER over CoPc and CoPc-THF.

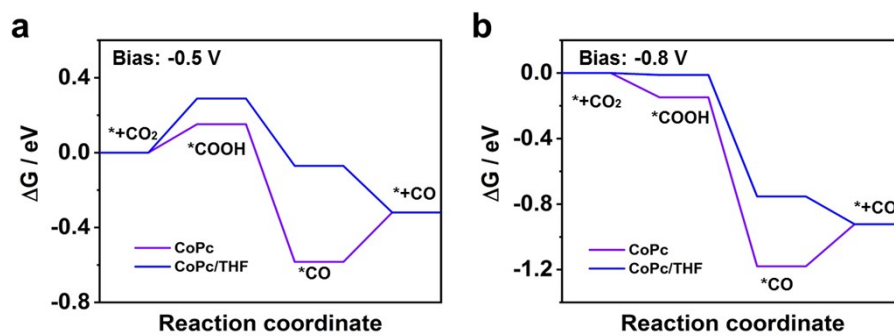


**Figure S18.** (a) Reaction Gibbs free energy diagrams for CO<sub>2</sub>RR to CO on CoPc and CoPc-THF after applying a -0.5 V bias potential. (b) Reaction Gibbs free energy diagrams for CO<sub>2</sub>RR to CO on CoPc and CoPc-THF after applying a -0.8 V bias potential.



**Table S1.** Comparison of n-propanol in CO<sub>2</sub>RR on various Cu-based catalysts.

Samples	FE of n-propanol(%)	Partial current density of n-propanol (mA cm <sup>-2</sup> )	References
CoPc/THF/Cu	16.8	28.56	This work
OD-Cu	10.07	18	This work
Cu <sub>DS</sub>	15	15	S6
CuSx-DSV	3.8	9.9	S7

**Table S2.** Structural parameters of CoPc/X extracted from the EXAFS fitting. ( $S_0^2=0.80$ )

Sample	Scattering		R(Å)	$\sigma^2(10^{-3}\text{Å}^2)$	$\Delta E_0(\text{eV})$
	pair	CN			
CoPc	Co-N	4.0*			
CoPc/THF	Co-N	3.8±0.6	1.95±0.02		
	Co-O	0.6±0.4	1.93±0.02	5.0±0.5	-4.4±0.3

$S_0^2$  is the amplitude reduction factor  $S_0^2=0.8$ ; CN is the coordination number; R is interatomic distance (the bond length between central atoms and surrounding coordination atoms);  $\sigma^2$  is Debye-Waller factor (a measure of thermal and static disorder in absorber-scatterer distances);  $\Delta E_0$  is edge-energy shift (the difference between the zero kinetic energy value of the sample and that of the theoretical model). R factor is used to value the goodness of the fitting.

## References

- S1 J. J. Lv, M. Jouny, W. Luc, W. Zhu, J. J. Zhu, F. Jiao, *Adv. Mater.* **2018**, *30*, e1803111.
- S2 C. Chen, X. Yan, S. Liu, Y. Wu, Q. Wan, X. Sun, Q. Zhu, H. Liu, J. Ma, L. Zheng, H. Wu, B. Han, *Angew. Chem. Int. Ed.* **2020**, *132*, 16601-16606.
- S3 G. Kresse, J. Furthmüller, *Phys. Rev. B* **1996**, *54*, 11169.
- S4 P. E. Blöchl, *Phys. Rev. B* **1994**, *50*, 17953
- S5 J. P. Perdew, K. Burke, M. Ernzerhof, *Phys. Rev. Lett.* 1996, *77*, 3865.
- S6 Z. Gu, H. Shen, Z. Chen, Y. Yang, C. Yang, Y. Ji, Y. Wang, C. Zhu, J. Liu, J. Li, T.-K. Sham, X. Xu, G. Zheng, *Joule* 2021, *5*, 429-440.
- S7 C. Peng, G. Luo, J. Zhang, M. Chen, Z. Wang, T.-K. Sham, L. Zhang, Y. Li, G. Zheng, *Nat. Commun.* **2021**, *12*, 1580.